Journal of Chromatography, 548 (1991) 61–79
Elsevier Science Publishers B.V., Amsterdam

CHROMSYMP. 2319

Multivalent ion-exchange model of biopolymer chromatography for mass overload conditions

PIOTR CYSEWSKI

Akademia Medyczna w Bydgoszczy, Zakład Chemii Fizycznej, M. Skłodowskiej-Curie 9, 85-094 Bydgoszcz (Poland)

ALAIN JAULMES, RAMONA LEMQUE, BERNARD SÉBILLE and CLAIRE VIDAL-MADJAR*

Laboratoire de Physico-Chimie des Biopolymères, C.N.R.S., Université Paris-Val-de-Marne, 2 Rue Henry Dunant, 94320 Thiais (France)

and

GERD JILGE[a]

Institut für Anorganische Chemie und Analytische Chemie, Johannes Gutenberg-Universität, W-6500 Mainz (Germany)

ABSTRACT

The simple model of multivalent ion-exchange biopolymer chromatography is analyzed on the basis of classical quasi-chemical treatments. The rigorous isotherm equation deduced from the stoichiometric displacement model (SDM) was used to stimulate the migration of a solute through the chromatographic column in the isocratic and gradient elution modes. The peak profiles generated for various sample sizes were compared with those obtained on the basis of a Langmuir isotherm. Peak tailing increases with the value of the exponent Z, defined as the ratio of the protein valency to the displacing counter-ion valency. For large Z the asymmetries due to the non-linearity of the isotherm are still present for small sample sizes, but may be reduced by using a displacing counter ion of higher valency. To illustrate the theoretical results, the ion-exchange model was applied to analyse the zonal elution behaviour of bovine serum albumin on a polymeric anion-exchange stationary phase deposited on silica. The effective charge of the protein ($m = 8$) was determined at infinite dilution with mono- and a divalent counter-ions. This value was introduced into the SDM isotherm to predict the elution behaviours in mass-overload conditions and the maximum loading capacity of the protein was determined. Good agreement between theory and experiment was obtained: for about the same capacity factor at infinite dilution, a larger peak asymmetry due to non-linear effects is found with a monovalent counter ion.

INTRODUCTION

High-performance ion-exchange chromatography (HPIEC) is being increasingly used for protein separations on both analytical and preparative scales. The stoichiometric displacement model (SDM) was successfully applied to predict the HPIEC retention behaviour at infinite dilution of a wide variety of biopolymers [1–3].

[a] Present address: Boehringer Ingelheim GmbH, W-6507 Ingelheim, Germany.

0021-9673/91/$03.50

It considers electrostatic interactions and is derived from the simple laws of mass action expressing the chemical equilibria between the interacting species [4].

Although the most important interactions involved in ion-exchange chromatography are electrostatic interactions between charged centres ruled by the simple Coulomb law, the retention behaviour is much more complex [5,6]. The complicated three-dimensional biopolymer structure, the unknown charge distribution, the amphoteric character of the protein and the heterogeneity of the support are the main reasons for difficulties in acquiring a proper understanding of the retention and binding behaviour of proteins. However, the SDM has been tested for a large number of HPIEC systems at infinite solute dilution and accounts well for retention volume variations with the displacer salt concentration. The model was recently improved to take hydrophobic interactions into account and to explain why the retentions observed at high salt concentrations deviate from those predicted by the SDM theory [7].

Starting from the simple SDM hypothesis, the adsorption of proteins on ion-exchange supports was explained by the multivalent ion-exchange scheme of Velayudhan and Horváth [8] and by the mass-action model of Whitley and co-workers [9,10]. The adsorption isotherms show strong curvature depending on the valency of the studied protein or the charge of the counter ion of the displacing salt. As retention volumes and peak shapes in non-linear chromatography are mainly governed by the adsorption isotherm [11], strong retention shifts and peak distortions are to be expected in the HPIEC of proteins at finite solute concentrations.

As HPIEC is being increasingly used for preparative purposes [12], it is useful to be able to predict the elution behaviour of proteins in mass-overload conditions to optimize separations [13–15]. The aim of this paper is to give an explicit presentation of the ion-exchange adsorption model and to apply it to numerical simulations of the ion-exchange chromatographic process.

Although the SDM model has been successfully applied to predict the retention of proteins on ion-exchange supports at infinite dilution, the simulations for mass-overload conditions were all limited to a Langmuir isotherm [10,13,14] or a two-site Langmuir-type isotherm [15]. Until now the rigorous form of the ion-exchange isotherm has not been used because it has the drawback of being an explicit form of the solute concentration as a function of the amount adsorbed. A Langmuir model was often found to fit well the adsorption protein data on ion exchangers [9], but it is unable to describe the dependence on salt concentration.

Therefore, simulations based on the rigorous SDM isotherm are useful for a better understanding of the HPIEC behaviour of proteins and for optimizing separations in mass-overload conditions using linear or gradient elution. To illustrate the theoretical results obtained with an SDM isotherm, the ion-exchange model was applied to analyse the zonal elution behaviour of bovine serum albumin (BSA) on a weak anion-exchange HPIEC support, *viz.*, a copolymer of vinylimidazole and vinylpyrrolidone (PVP–PVI) deposited on silica.

THEORETICAL

Let us consider the equilibrium of the system consisting of a liquid biopolymer solution and a solid ion-exchange particle. We assume the following:

the deviations from ideality of the protein solutions are small and concentration

is a sufficient measure of their activity, which means that activity coefficients ara equal to unity in the whole concentration range; this fairly crude assumption is extensively accepted [1–10];

protein adsorption has a multi-point nature, which has been shown experimentally, for example, by Jennissen [16];

the properties of biopolymer molecules (charge, valency, structure, size, etc.) do not change during the ion-exchange process;

solid adsorbents must have a wide-pore and homogeneous nature although significant deviations from such an ideal model are observed in experimental investigations;

the particle adsorption properties are represented by active adsorption centres which are entirely covered by co-ions; and

the adsorption of proteins has a competitive character and their binding to the surface is accompanied by simultaneous desorption of an equivalent amount of salt counter ions.

Ion-exchange adsorption isotherm

The process of ion-exchange adsorption–desorption equilibria may be represented by the following expression

$$n\mathrm{PB}_{r+m} + m\mathrm{X}_n\mathrm{A} \rightleftharpoons n\mathrm{X}_m\mathrm{PB}_r + m\mathrm{A}^{n-} + nm\mathrm{B}^{+} \tag{1}$$

where P symbolizes the protein molecule, X the part of the solid surface containing one adsorption site and A and B are ions with charges of opposite signs relative to particle and protein, respectively. The numbers of bonds in all complexes are indicated by appropriate subscripts, as in usual chemical formulae. The salt counter ion is n-valent, the protein molecule is m-valent towards particles and has a total charge $r + m$. The chemical equilibria are given for anion-exchange chromatography, but may easily be adapted, as well as all further developments, for cation-exchange chromatography.

The law of mass action for the ion-exchange process may be given as

$$K' = \frac{\{\mathrm{X}_m\mathrm{PB}_r\}^n[\mathrm{A}^{n-}]^m[\mathrm{B}^{+}]^{mn}}{[\mathrm{PB}_{r+m}]^n\{\mathrm{X}_n\mathrm{A}\}^m} \tag{2}$$

where K' is given in terms of volumetric and surface concentrations and brackets [ ] and braces { } represent the concentrations of the given species in bulk-phase solutions (mol/l) and in the adsorbed state (mol/m^2), respectively. In general, the protein molecule is a poly-ion interacting with a given number of co-ions in solution and must undergo the multivalent dissociation process. It is possible to write the set of chemical equations for the equilibrium state

$$\mathrm{PB}_k \rightleftharpoons \mathrm{PB}_{k-1}^{-} + \mathrm{B}^{+} \rightleftharpoons \ldots \rightleftharpoons \mathrm{P}^{k-} + k\mathrm{B}^{+} \tag{3}$$

where k is the maximum number of ions interacting with protein and is equal to the total surface charge of protein. Of course, the probabilities of the various complexes

are not identical. The given equilibrium conditions determine all the concentrations. The set 3 can be written in a simple way (for $k = r + m$)

$$PB_{r+m} \rightleftharpoons PB_r^{m-} + mB^+ \tag{4}$$

the equilibrium constant of which is as follows

$$K'' = \frac{[PB_r^{m-}][B^+]^m}{[PB_{r+m}]} \tag{5}$$

If we combine eqns. 2 and 5, we obtain

$$K = \frac{\{X_mPB_r\}^n[A^{n-}]^m}{[PB_r^{m-}]^n\{X_nA\}^m} \tag{6}$$

where $K = K'/(K'')^n$ is related to the equilibrium

$$nPB_r^{m-} + mX_nA \rightleftharpoons nX_mPB_r + mA^{n-} \tag{7}$$

The total number of available sites for adsorption, Q_X, may be expressed as the sum of the sites taken by protein, mQ_P, and those taken by the salt counter ions

$$Q_X = nS\{X_nA\} + mQ_P \tag{8}$$

where S is the total interfacial surface area and $Q_P = S\{X_mPB_r\}$ is the amount of adsorbed protein.

We may now write the isotherm equation by substituting eqn. 8 into eqn. 6 and simple rearrangement

$$[PB_r^{m-}] = \frac{Q_P}{L}\left(\frac{[A^{n-}]}{Q_X - mQ_P}\right)^Z \tag{9}$$

where $Z = m/n$, $L = SK^{1/n}/(nS)^Z$ and Q_X/m is the maximum protein loading capacity. The above isotherm is a complex expression of the concentration as a function of the adsorbed amount. In general, the adsorbed amount cannot be expressed as a function of solute concentration but, of course, may be calculated by numerical means.

In the case of equal valencies for the protein and salt counter ion, Z is equal to unity and the isotherm is of the Langmuir type

$$Q_P = \frac{Q_X}{m} \cdot \frac{K_1[PB_r^{m-}]}{[A^{n-}] + K_1[PB_r^{m-}]} \tag{10}$$

where $K_1 = K^{1/n}$. For some given experimental conditions, m may be equal to the valency of the displacing salt, n, as the charge of the protein is usually ruled by the pH of the medium. However, with the experimental conditions used for ion-exchange separations, this situation is unrealistic, the number Z determined with monovalent displacing counter ions generally being larger than 3 [7].

For extremely low concentrations, eqn. 9 becomes of the Henry isotherm type

$$Q_P = LQ_X^z \cdot \frac{[PB_r^{m-}]}{[A^{n-}]^z} \tag{11}$$

The retention volume may be related to the isotherm parameters by the well known relationship

$$k' = V_{(C\to 0)}^R/V_0 - 1 = \frac{1}{V_0}\left(\frac{dQ_P}{dC}\right)_{C=0} \tag{12}$$

where C is the protein concentration and V_0 the volume of the mobile phase. Using eqn. 9 leads to

$$k' = \frac{Q_X^z}{V_0 R} \tag{13}$$

where $R = [A^{n-}]^z/L$. One obtains here the same expression as that found for the SDM of Regnier and co-workers [1–3], which relates the retention volume at infinite dilution to the displacing-salt concentration.

Numerical simulation method

The theoretical propagation differential equation describing the solute mass balance may be written as

$$\frac{\partial C}{\partial t} + u \cdot \frac{\partial C}{\partial z} + \frac{1}{\Delta v_0} \cdot \frac{\partial q}{\partial t} = D' \cdot \frac{\partial^2 C}{\partial z^2} \tag{14}$$

where q is the amount of solute adsorbed in an infinitesimal cross-slice of column and Δv_0 is the corresponding mobile phase volume. One uses the abscissa, z, along the column length, the time, t, elapsed from the moment of injection, the mobile phase velocity, u, and the solute concentration, C. D' is a global dispersion coefficient accounting for all the contributions to the dispersive effect.

The equilibrium is assumed to be reached at any time, so that C is a function of q according to eqn. 9, which may be written in the form

$$C = \Omega \cdot \frac{q}{(q_X - mq)^z} \tag{15}$$

where q_X is the number of binding sites on the solid phase for the infinitesimal cross-slice and Ω is a function of $[A^{n-}]$

$$\Omega = \frac{(n\Delta S)^z}{\Delta S K^{1/n}} \tag{16}$$

ΔS is the adsorbing surface area in the slice. A stepwise numerical method was used to solve the system given by eqns. 14 and 15.

Mobile phase progression and Fick's law. The band broadening is due to various terms such as the diffusion in the mobile phase, the flow non-uniformity and the kinetic mass-transfers. As a first approximation we assume that all these effects are included in the global dispersion coefficient D'. In HPLC experiments the axial diffusion in the mobile phase and the eddy diffusion can usually be neglected, but slow mass-transfer kinetics are the main contribution to the large theoretical plate heights often observed for the elution of proteins in the isocratic mode. A rigorous numerical procedure should account for slow mass-transfer kinetics separately [10,17]. However, for the column efficiencies generally used in protein separations, one may approximate the kinetic contribution with the global dispersive term. We have shown [17] that the limit for this approximation is close to a theoretical plate number of 15; the approximation leads to a 5% deviation for the retention time at the peak maximum and a 10% deviation for the peak width.

Several methods for solving the differential equation (eqn. 14) in the presence of a Langmuir-type isotherm and axial dispersion have been described: algorithms were supplied as standard subroutines to simulate isocratic elution [18,19] and linear gradient elution [13]; Lin *et al.* [20] suggested the Lax–Wendroff scheme; Phillips *et al.* [19] employed a finite difference technique where a global first-order law includes mass-transfer kinetics.

The approach adopted here combines the Craig method [14,15], which divides the column into a series of discrete stages, and the finite difference technique. As shown previously [17], this more versatile algorithm enables one to combine axial dispersive effects with any kinetic law for solute mass-transfers. Moreover, the method is not limited to the simulation of peak profiles with linear solvent gradients but permits gradients of arbitrary shape to be considered.

The column is assumed to be divided into slices of thickness Δz. Fick's law, expressed as

$$\Phi = -\Sigma D' \cdot \frac{\partial C}{\partial z} \tag{17}$$

is approximated by

$$\Phi = -\Sigma D' \cdot \frac{\Delta C}{\Delta z} \tag{18}$$

where Σ is the cross-sectional area of the liquid phase and Φ is the molar rate of solute "exchanged" by dispersion between two adjacent slices. It can be defined by the equation

$$\Phi = -\Delta v_0 \cdot \frac{\Delta_f C}{\Delta t} \tag{19}$$

where $\Delta_f C$ is the resulting partial concentration change in a slice during the time interval Δt necessary to the liquid phase to flow from one slice to the following one

$$\Delta z/\Delta t = u \tag{20}$$

We calculate $\Delta_f C = -\Phi \Delta t / \Delta v_0 = -\Phi / u\Sigma$. Here $\Delta_f C = (D'/u)(\Delta C/\Delta z) = \Delta CF$, where $F = D'/u\Delta z$ is a factor independent of z or t.

Thus Fick's law can be written for the extreme slices

$$\left.\begin{aligned} \Delta_f C(\Delta z,t) &\approx F[C(2\Delta z,t) - C(\Delta z,t)] \\ \Delta_f C(L,t) &\approx F[C(L - \Delta z,t) - C(L,t)] \end{aligned}\right\} \tag{21}$$

and for the inner slices

$$\left.\begin{aligned} \Delta_f' C(z,t) &= \Delta_f C(z,t) - \Delta_f C(z - \Delta z,t) \\ &= F\{C(z + \Delta z,t) - C(z,t) - [C(z,t) - C(z - \Delta z,t)]\} \\ &= F[C(z + \Delta z,t) - 2C(z,t) + C(z - \Delta z,t)] \end{aligned}\right\} \tag{22}$$

To ensure the convergence of the numerical procedure, Δt may be subdivided into fractions and the changes subsequently added for every slice.

The mobile phase progression is rendered by a mere index shift of the mobile phase concentrations in the slices.

Sorption equilibrium inside a given slice. We assume that the equilibrium takes place as soon as the two new fractions meet in a given slice: thus $q(z,t)$ and $C(z - \Delta z,t)$ will originate the new values $q(z,t + \Delta t)$ and $C(z,t + \Delta t)$.

The initial values q_0 and C_0 give the total amount of solute in the slice: $s = q_0 + \Delta v_0 C_0$, which will be equal to the final amount, $\bar{q} + \Delta v_0 \bar{C}$, at equilibrium.

As

$$\bar{C} = \Omega \cdot \frac{\bar{q}}{(q_X - m\bar{q})^z} \tag{23}$$

one can write

$$\bar{q} + \frac{\Delta v_0}{R} \cdot \frac{\bar{q}}{(q_X - m\bar{q})^z} - q_0 - \Delta v_0 C_0 = 0 \tag{24}$$

A step interpolation will yield the value of $\bar{q}$, from which one can deduce $\bar{C}$ according to the equation

$$\bar{C} = C_0 + \frac{q_0 - \bar{q}}{\Delta v_0} \tag{25}$$

The method described above has two interesting features: it is built to ensure mass conservation all through the simulated chromatographic process and the thickness of the slices may be chosen as low as desirable to approach close to the actual physical phenomena.

Case of gradient elution. The concentration of counter ions, $[A^{n-}]$, is an arbitrary function of the quantity $y = z - ut$. For example it may be either:

(1) a linear function

$$\left.\begin{aligned}[A^{n-}] &= C_C^0 + Gy \text{ (for } y \geqslant 0)\\ [A^{n-}] &= C_C^0 \quad\quad \text{(for } y \leqslant 0)\end{aligned}\right\} \tag{26}$$

with which assumption, at any point of the column,

$$[A^{n-}] = C_C^0 + GyY(y) \tag{27}$$

where the step Dirac function Y is 1 for $y > 0$ and 0 for $y \leqslant 0$,

(2) or a parabolic function

$$\left.\begin{aligned}[A^{n-}] &= C_C^0 + Gy + \frac{B}{2}y^2 \text{ (for } y \geqslant 0)\\ [A^{n-}] &= C_C^0 \quad\quad\quad\quad\quad\quad \text{(for } y \leqslant 0)\end{aligned}\right\} \tag{28}$$

EXPERIMENTAL

Materials

The reagents used for the stationary phase synthesis were N-vinylimidazole, vinylpyrrolidone and 1,4-butanediol diglycidyl ether, purchased from Janseen Chimica (Beerse, Belgium).

The silica support (LiChrospher Si-300) (particle diameter $d_p = 10\ \mu m$ and pore size 300 Å) was purchased from Merck (Darmstadt, Germany).

The protein used for the chromatographic study, BSA monomer, was obtained from Sigma (St. Louis, MO, USA). The buffer was Tris, obtained from Aldrich-Chemie (Steinheim, Germany).

Chromatography

The chromatographic system consisted of a pump (HPLC PUMP 420, Kontron Instruments, Zurich, Switzerland) and a UV detector (Model SPD-6A, Shimadzu, Kyoto, Japan) operating at 280 nm. A sample injector (Model 7125, Rheodyne, Berkeley, CA, USA) with a 20-μl sample loop was used. To determine the ion-exchange capacity, frontal loading was performed with a 2-ml sample loop and the displacing salt elution was monitored at 256 nm.

The chromatographic packing was a polymeric anion-exchange stationary phase deposited on silica. The polymer used was a PVP–PVI copolymer (75:25) cross-linked with 1,4-butanediol diglycidyl ether (BUDGE). It was synthesized using the one-step polymer-coating method developed by Sébille and co-workers [21,22].

The specific anion-exchange capacity of the adsorbent per unit volume of mobile phase was 0.15 mequiv./ml. It was determined by frontal loading with sodium chloride as the eluent and sodium nitrate as the displacing agent.

The chromatographic column (100 × 41 mm I.D.) was slurry packed. The column temperature was maintained at 10°C during the experiments using a thermostated water-bath. The eluent used was 20 m*M* Tris buffer (pH 7.5). For the isocratic elution, the ionic strength was imposed by a monovalent (NaCl) or a divalent salt

(Na_2SO_4). The capacity factor for infinite dilution, k', was calculated by reference to the retention volume of an unretained protein, α-chymotrypsinogen A.

Computer system

The analogue output of the detector was connected to a digital voltmeter (Model 3497; Hewlett-Packard, Palo Alto, CA, USA). The data (4 digits precision) were stored on floppy disk and analysed with a personal computer (Compaq Deskpro, Model 386/20e) equipped with an arithmetic coprocessor.

The simulations were performed in Pascal language. The step Δz used for calculations was 0.05 cm. A numerical dispersion contributed to the broadening of the elution peak [23]; its contribution to the plate height was $H_N = 0.05$ cm.

RESULTS AND DISCUSSION

Numerical simulations

For comparison with a Langmuir-type isotherm, various isotherms generated with eqn. 9 and increasing values of $Z = m$ are given in Fig. 1. All the isotherms have the same slope at the origin ($k' = 10$). The solute maximum loading capacity (dashed line for each Z value) is equal to the ion-exchange capacity available for adsorption divided by m. The curvature of the isotherm at the origin increases with increasing $Z = m$ value and the derivative of the isotherm reaches zero for lower solute concentrations

$$k'' = \frac{1}{V_0}\left(\frac{d^2Q_P}{dC^2}\right)_{C=0} = -\frac{2\,m\,z\,k'^2\,V_0}{Q_X} \tag{29}$$

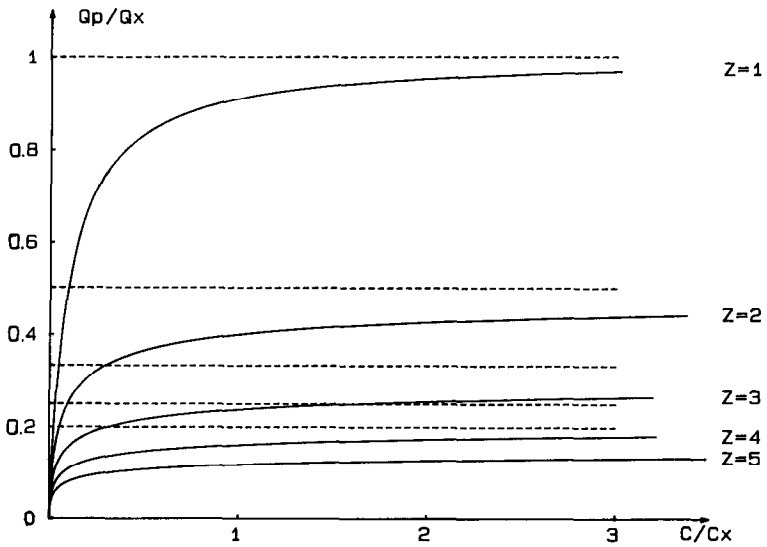

Fig. 1. Influence of exponent Z on the shape of SDM adsorption isotherm ($Z = m$), with equal slopes at the origin ($k' = 10$).

It may therefore be predicted, on the basis of the SDM theory, that the range for linear chromatography will be limited at large m values and strongly tailing peaks will be observed in the isocratic elution mode at much lower concentrations than with a Langmuir isotherm.

The isotherms of Fig. 1 were used to simulate the chromatographic behaviour with isocratic elution with a monovalent displacing ion. In Fig. 2 the theoretical profiles generated with increasing sample size and $m = Z = 5$ are compared with those obtained on the basis of a Langmuir isotherm ($Z = 1$). The simulations were performed with a fixed value of the solute capacity factor ($k' = 10$). This can be related to experiments where k' is kept constant by changing the displacing salt concentration. The results of the simulation are presented as a plot of the outlet solute concentration divided by the active site concentration ($C_X = Q_X/V_0$) *vs.* the reduced elution volume, $V(C)/V_0$. In this instance the dispersive coefficient was kept at a negligible value, but a dispersive effect arises from the numerical steps chosen for the calculation [23]. The corresponding contribution to the plate height is $H_N = 0.05$ cm.

For solute concentrations larger than $C_X/10$ the retention volume at the peak maximum is already close to V_0 when $m = Z = 5$. In agreement with theory [24], the

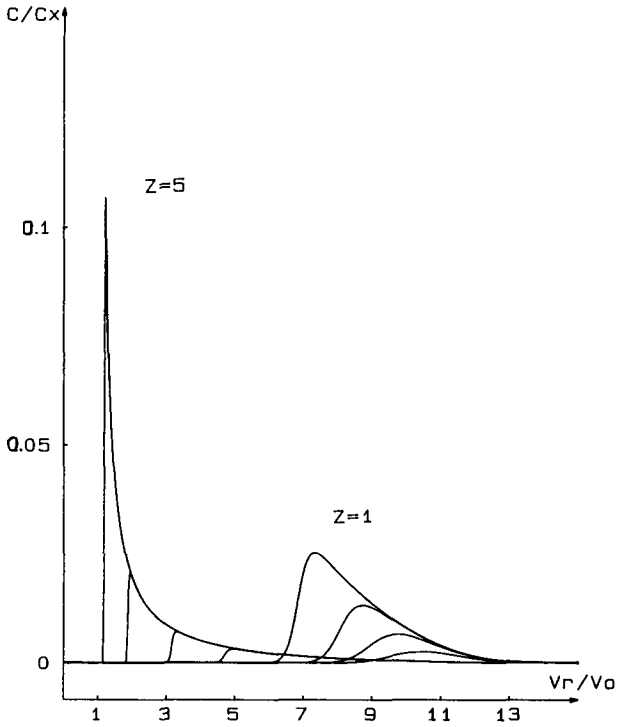

Fig. 2. Isocratic elution with a monovalent displacing salt. Comparison of the peak profiles simulated with a Langmuir isotherm and an SDM isotherm ($Z = 5$). Column length, 5 cm; flow-rate, 1 ml/min; sample volume, 0.020 ml; isocratic elution with $k' = 10$. Sample size: $Q_X/15$, $Q_X/30$, $Q_X/60$, $Q_X/120$.

rear part of the peak coincides with the derivative of a convex adsorption isotherm if the dispersive effects can be neglected

$$V(C) = V_0 + \frac{dQ_P}{dC} \tag{30}$$

The influence of the dispersive effect on the elution peaks generated with $m = Z = 5$ is shown in Fig. 3. In spite of the larger dispersion coefficients used for the simulations, corresponding to the plate-height contributions $H_D = 0.12$ cm and $H_D = 0.6$ cm (Fig. 3a and b), the retention volume at the peak maximum is still well predicted by the first derivative of the adsorption isotherm (dotted line).

These results show that, with isocratic elution and under mass-overload conditions, non-linear effects dramatically control the retention process of solutes with large effective charge number. With larger values of the charge of the solute, m, the curvature at the origin increases (eqn. 29) and generates strong tailings with a shift towards lower retention volumes [11].

For a solute with a given charge number ($m = 6$), Fig. 4 illustrates the influence of non-linear effects with counter ions of various valencies. The capacity factor at

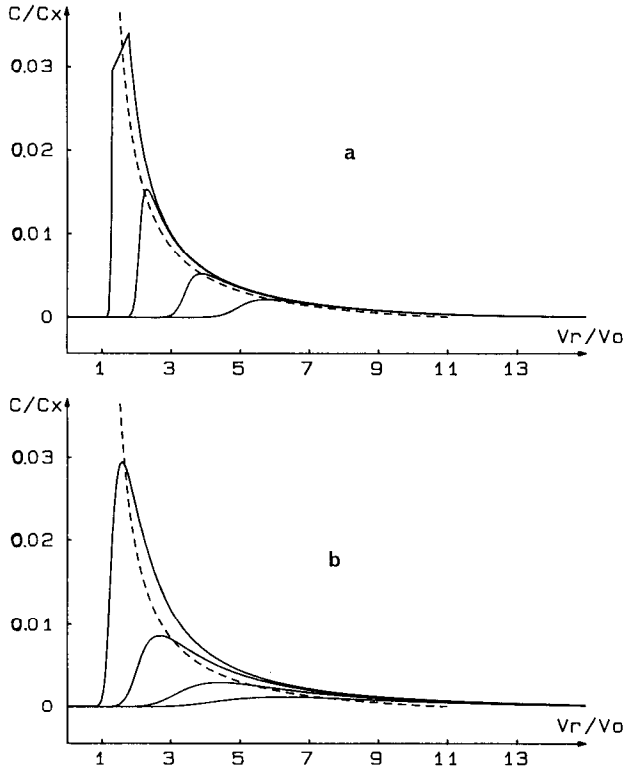

Fig. 3. Influence of the dispersive effects on the peak shapes generated with $Z = 5$ (SDM isotherm). Same conditions as in Fig. 2 and (a) $D' = 0.010$ cm^2/s, $H_D = 0.12$ cm; (b) $D' = 0.050$ cm^2/s, $H_D = 0.60$ cm. Dashed lines, first derivative of the adsorption isotherm.

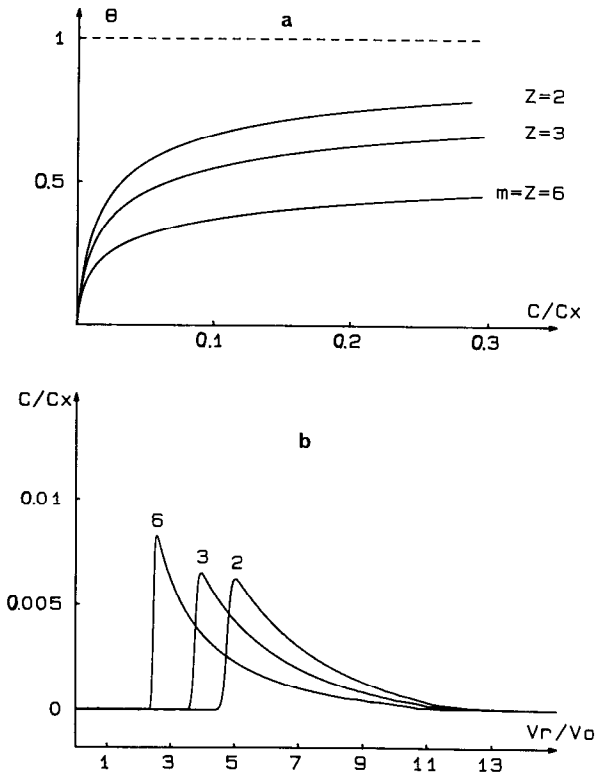

Fig. 4. Influence of the valency of the counter ion on the isocratic elution of a solute with six effective charges. (a) SDM isotherm; (b) peak profiles simulated with an SDM isotherm. Exponent $Z = 2, 3, 6$. Same conditions as in Fig. 2 with sample size $Q_X/60$.

infinite dilution remained constant for the simulated profiles ($k' = 10$). As predicted from eqn. 29, the tailing due to the overload effects increases with increasing valency of the displacer ion used in the eluent. This result shows that a displacing counter ion of larger valency should be used in order to reduce mass-overload effects in the isocratic elution mode.

This conclusion is of limited application in practice, however: because of the high selectivity of the supports, linear gradient elution is most commonly used for protein separations by HPIEC, in order to reduce band broadening. A model was described [25] that predicts the separation of proteins at infinite dilution, with a linear salt gradient. Antia and Horváth [13] studied the effect of gradient elution and column overload on the separation of a binary mixture with a numerical procedure, but their simulations were limited to isotherms of the Langmuir type.

Because of the significant differences observed between the simulations performed with isocratic elution in the cases of an SDM isotherm and a Langmuir isotherm (Fig. 2), it is interesting to examine the influence of the valency of the counter ion in gradient elution on the elution profile of a solute with a given value of the charge, m. To compare with the simulations in the isocratic mode in Fig. 4, the solute charge is

6 and for each Z the slope of the gradients was selected so as to obtain the end of the rear edge of the peak at $V_r/V_0 \approx 11$ (Fig. 5). The initial value of k' at the gradient beginning is 100: this would correspond to experiments where the initial concentration of the displacing salt is adjusted to give $k' = 100$. As already shown with simulations assuming a Langmuir isotherm [13], gradients strongly reduce the asymmetry owing to the non-linearity of the isotherm. With a linear salt gradient (Fig. 5a), the mass-overload effects increase with displacing counter ions of lower valency.

Although not very realistic, but for illustrating the versatility of the present algorithm, Fig. 5b shows the profiles obtained with a parabolic gradient simulating salt concentrations increasing with time. For comparison with the peaks in Fig. 5a, the initial slope at the origin was set to a value equal to the slope of the linear gradient. The front of the peak is eluted at a slightly lower retention volume, and the peak tailing is much reduced, especially when a monovalent displacing ion is assumed for the simulations. Of course, other types of gradient functions could have been used, such as a linear one ending with a plateau.

These simulations based on the rigorous SDM isotherm predict, for a pure

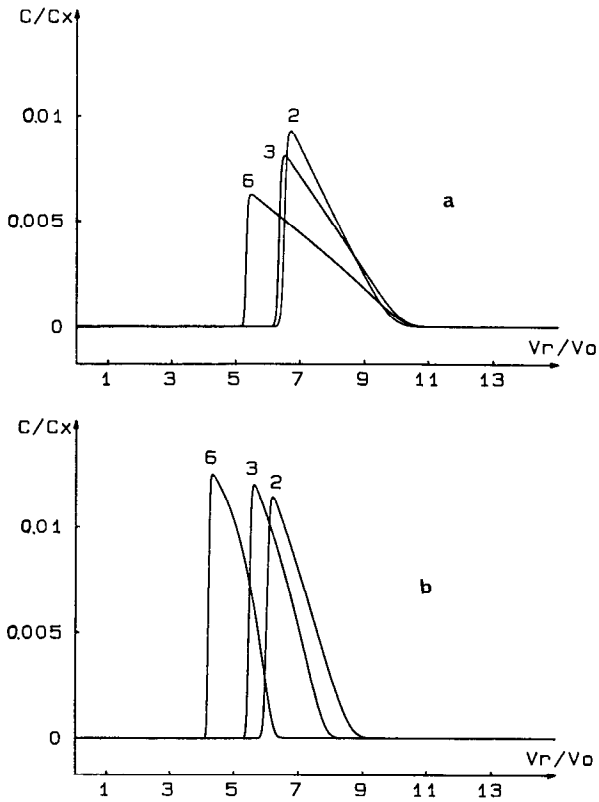

Fig. 5. Influence of the valency of the counter ion on the gradient elution of a solute with six effective charges. (a) Linear gradient; (b) parabolic gradient ($B/C_X = 2.10^{-5}\,s^{-2}$). $Z = 2$, $G/C_X = 0.017\,s^{-1}$; $Z = 3$, $G/C_X = 0.008\,s^{-1}$; $Z = 6$, $G/C_X = 0.003\,s^{-1}$. Same conditions as in Fig. 2 with sample size $Q_X/60$. Initial value of $k' = 100$.

ion-exchange mechanism, more important non-linearity effects with proteins of larger effective charge, but a decrease in mass-overload effects is to be expected with a displacing counter ion of higher valency.

HPIEC study of BSA with isocratic elution

To illustrate the previous theoretical simulations, we studied the chromatographic behaviour of BSA eluted from an anion-exchange column under mass-overload conditions. This protein was selected to test the model as the adsorption of BSA on the anion-exchange support, a PVP–PVI (75:25) copolymer deposited on silica, is described by an isotherm of convex shape.

In order to determine the exponent, Z, retention studies were first performed in the linear range of the adsorption isotherm and analysed with the SDM model for infinite dilution [1–3]. The capacity factor, k', extrapolated to zero sample size is related to the displacing counter ion concentration C_C, according to the equation

$$\log k' = a - Z \log C_C \tag{31}$$

Fig. 6 shows the variations of k' with the concentration of a mono- or a divalent salt. The values of Z were calculated by a linear regression analysis of plots of $\log k'$ *vs.* $\log C_C$. The Z value determined with sodium chloride as the displacing salt is 7.9 ± 0.4. With sodium sulphate the Z value is 4.1 ± 0.4. The errors are given for a 95% confidence interval. This result is in agreement with theory, the ratio Z being twice as large with chloride ions as that measured with sulphate ions.

The apparent Z values are generally considered to be mean values over all orientations of molecules on the surface [6]. Moreover, Z measurements may be affected by hydrophobic interactions [7] and its value may be non-integral when

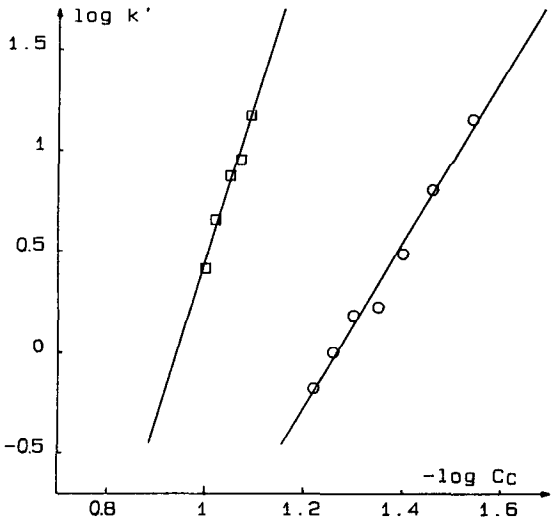

Fig. 6. Dependence of $\log k'$ on the log (salt concentration) for BSA on an anion exchanger, PVP–PVI on silica; flow-rate, 1 ml/min; eluent, 0.020 *M* Tris buffer (pH 7.5). (□) NaCl; (○) Na_2SO_4.

determined with a monovalent salt. With experimental conditions close to those used in this work, Melander *et al.* [7] measured values of Z of 3.55 and 2.99 for BSA eluted from a weak and a strong anion exchanger, respectively, with ammonium sulphate as the displacing salt. The value for the weak anion exchanger is close to that determined on PVP–PVI at pH 7.5 by varying the sodium sulphate concentration. The good agreement of the effective charge of the protein ($m = 8$) deduced from Z measurements with mono- and divalent displacing ions show that, with both salts, the retention is mainly governed by an ion-exchange mechanism. This value of m was selected to simulate the elution peaks under mass-overload conditions.

Fig. 7 illustrates the experimental profile of the BSA (dotted lines) with a displacing salt with a monovalent counter ion (sodium chloride) and a divalent counter ion (sodium sulphate). An impurity (about 10% of the total sample) is eluted on the tailing end of the main peak. For comparing peak shapes, we tried to fix the salt concentration so as to obtain k' values as close as possible for both displacing salts. This can only be partially achieved, as small variations in salt concentration induce

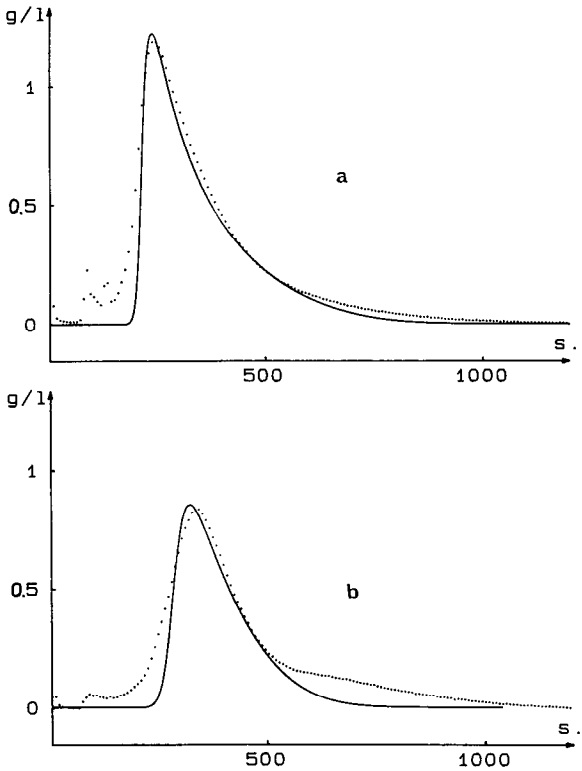

Fig. 7. Comparison of non-linear effects for BSA eluted with a mono- or a divalent counter ion from a PVP–PVI anion-exchange column. Eluent, 0.020 M Tris buffer (pH 7.5); flow-rate, 1 ml/min; column length, 10 cm; $V_0 = 1.2$ ml. Dotted lines, experimental values stored by computer data acquisition; solid lines, best fit of the simulated peak. $Q_X = 5.7$ mg; $D' = 0.015$ cm^2/s; $H_D = 0.22$ cm; $H_N = 0.05$ cm. (a) 80 mM NaCl, sample size 0.025 mg, $k' = 8$, $m = Z = 8$; (b) 35 mM Na_2SO_4, sample size 0.035 mg, $k' = 6.2$, $m = 8$, $Z = 4$.

large variations in the retention volume. The value of k' is 8 with sodium chloride (80 mM) and 6.2 with sodium sulphate (35 mM).

The theoretical profiles were fitted to the experimental profiles by fixing three parameters of the adsorption isotherm: k', m and Z. The plate height measured at infinite dilution is $H = 0.27$ cm. Taking into account the contribution to the plate height due to the numerical dispersion, H_N, the H value determines the contribution of the global dispersive effects, H_D, to be used in the simulations ($H = H_D + H_N$): simulations were performed with a global dispersive coefficient $D' = 0.015\ cm^2/s$. As usual with protein elution in the isocratic mode [5,22], the reduced plate height is large ($H/d_p = 270$). This poor efficiency is mainly due to slow mass-transfer kinetics such as the slow adsorption–desorption chemical exchanges and the restricted diffusion of BSA into the 300-Å pores of the support used.

The maximum loading capacity for the protein, Q_X/m, is the only parameter to be calculated from the best fit to the experimental profiles observed with a monovalent (Fig. 7a) and a divalent displacing ion (Fig. 7b). The maximum loading capacity per unit volume of mobile phase used in the simulations with both counter ions is $Q_X/mV_0 = 0.59$ mg/ml.

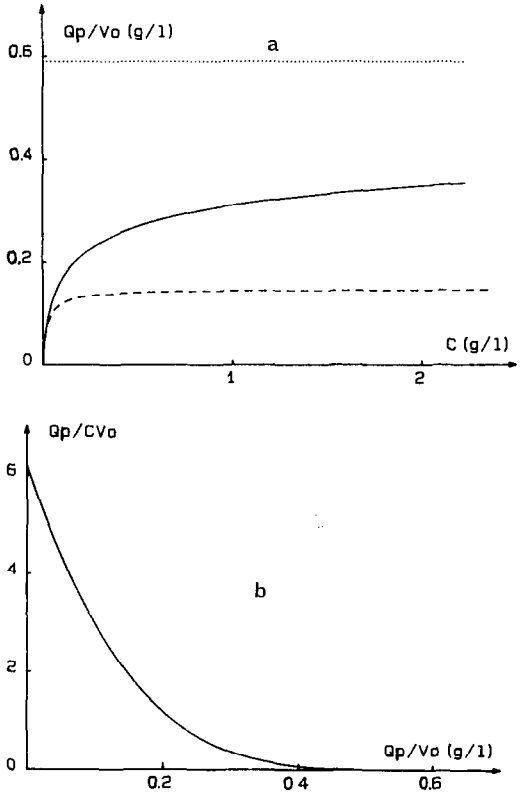

Fig. 8. Adsorption isotherm of BSA adsorbed on the PVP–PVI anion-exchange support in the presence of a divalent counter ion. Same experiment as in Fig. 7b ($k' = 6.2$; $k'' = -521$ l/g). (a) Solid line, SDM isotherm; dashed line, Langmuir isotherm; dotted line, $Q_X/mV_0 = 0.6$ mg/ml (protein loading capacity). (b) Scatchard plot corresponding to the SDM isotherm.

The experimental asymmetries determined from the ratio of half-widths measured at 20% of the peak height are 4.7 with sodium chloride (Fig. 7a) and 2.4 with sodium sulphate (Fig. 7b) in the mobile phase. The comparison of peak asymmetry may roughly be predicted by expanding $V(C)$ in first order near the origin (eqn. 30)

$$V(C) \approx V_0(1 + k' + k''C) \tag{32}$$

In the absence of dispersive effects and for small concentrations, the slope of the straight line defining the peak diffuse edge as $C = f(V)$ is equal to $1/(k''V_0)$. Therefore, a comparison of the asymmetries of the peaks in Fig. 7a and b could approximately be calculated from the ratio of these slopes, which for the present example is 3.3. This value is larger than the experimental value (2), which was determined from the ratio of the asymmetries measured at 20% of the peak maximum. The theoretical ratio would correspond to asymmetries measured near the baseline, but peak width determinations too close to the baseline would interfere with impurities. The comparison of the experimental asymmetries of BSA eluted with sodium chloride or sodium sulphate in the buffer is in good agreement with theory, which predicts an increase in peak tailing for mass-overload conditions when a monovalent ion is used as a displacer.

Fig. 8a shows the adsorption isotherm of BSA on the anion-exchange polymeric stationary phase in the presence of 35 mM sodium sulphate. The simulations in Fig. 7b were performed on the basis of this isotherm, with $m = 8$ and $Z = 4$. For comparison, the Langmuir isotherm (dotted line) with the same slope and curvature at the origin is given. Its protein maximum capacity is 32 times lower than that for the SDM isotherm, illustrated in Fig. 8a by a dotted line parallel to the concentration axis. Therefore, a Langmuir isotherm cannot be used to describe at the same time the adsorption behaviours at low and high protein concentrations in the solvent: the low concentration range determines the slope of the isotherm at the origin of the capacity factor. At high concentrations, the maximum loading capacity is reached very progressively in the case of an SDM isotherm with a large Z exponent and this is related to the overload effects observed in chromatography.

Fitting a Langmuir or a sum of two Langmuir isotherms to the experimental data for proteins adsorbed on an ion exchanger may lead to erroneous conclusions, as shown from the Scatchard plot in Fig. 8b. From this plot, one may conclude that the support is heterogeneous with adsorption on two different kinds of sites. The corresponding model, a sum of two Langmuir isotherms, is of course a wrong interpretation: the isotherm is of the SDM type (eqn. 9) and an exponent Z different from unity is responsible of the curvature of the Scatchard plot.

CONCLUSIONS

This study has shown that the rigorous isotherm derived from the law of mass action should be used to analyse the experimental adsorption data by an ion-exchange mechanism. For experiments determining directly the amount adsorbed as a function of concentration, such as frontal elution, the Scatchard plot may lead to the misinterpretation of results such as the existence of two kinds of sites. In contrast, a plot of $(Q_P/CV_0)^{1/Z}$ *vs.* Q_P should be used, the exponent Z being determined independently with the SDM model, extrapolated to zero surface coverage (eqn. 31).

Similarly, the parameter Z and the charge of the protein determined at infinite dilution should be introduced into the SDM isotherm equation to analyse or simulate non-linear effects in zonal elution on an ion-exchange support. This approach was used in this work and led to the prediction that peak tailing due to column overloading may be reduced by using a counter ion of higher valency. This conclusion may be useful for optimizing separations in preparative chromatography.

The theoretical results are in good agreement with experiments to analyse the non-linear elution behaviour of BSA on an anion exchanger. The above conclusions are not necessarily valid with other experimental systems, however: a pure ion-exchange mechanism is not often encountered in practice. Although the SDM theory predicts well the HPIEC retentions of many proteins at infinite dilution in most instances, it does not describe the elution behaviours of proteins at finite solute concentrations, because the model does not account for hydrophobic or self-association effects.

The multivalent ion-exchange theory is a first step in studying the adsorption mechanism of proteins on ion-exchange supports. It gives a simple tool for understanding the nature of the protein adsorption behaviour: a comparison of the elution profiles predicted on the basis of the SDM theory and the experimental profiles will give information about the nature of the adsorption process.

We are still far from a reliable explanation of all the characteristics of HPIEC and further investigations are necessary. The following aspects of the properties of HPIEC should be taken into account:

—the association–dissociation equilibria between protein molecules in both bulk and surface phases;

—the non-homogeneous character of the charge distribution both on the support surface and on the biopolymer molecule;

—the three dimensional structure of the protein, which may be changed during the binding process, and also the changes in the number of sites occupied by one biopolymer molecule, which means that the change in the value of m as a function of concentration must be considered;

—irreversible adsorption and the presence of pores of various sizes and shapes; and

—the modification of the support charge characterized by the adsorption–desorption of protein.

These are only a few features which should be considered in subsequent models to account for the complexity of HPIEC phenomena. Finally, the generalization to the multi-component case could be useful for optimizing the experimental conditions for the separation of proteins by preparative HPIEC.

ACKNOWLEDGEMENT

We gratefully thank the University of Paris-Val de Marne for the financial support, which allowed P.C. to collaborate with the CNRS Laboratory in Thiais.

REFERENCES

1 M. A. Rounds and F. E. Regnier, *J. Chromatogr.*, 283 (1984) 37.
2 W. Kopaciewicz, M. A. Rounds, J. Fausnaugh and F. E. Regnier, *J. Chromatogr.*, 266 (1983) 3.
3 R. R. Drager and F. E. Regnier, *J. Chromatogr.*, 359 (1986) 147.
4 A. Velayudhan and Cs. Horváth, *J. Chromatogr.*, 367 (1986) 160.
5 M. T. W. Hearn, A. N. Hodder and M. I. Aguilar, *J. Chromatogr.*, 443 (1987) 97.
6 M. T. W. Hearn, A. N. Hodder and M. I. Aguilar, *J. Chromatogr.*, 458 (1988) 45.
7 W. R. Melander, Z. El Rassi and Cs. Horváth, *J. Chromatogr.*, 469 (1989) 3.
8 A. Velayudhan and Cs. Horváth, *J. Chromatogr.*, 443 (1988) 13.
9 R. D. Whitley, R. Wachter, F. Liu and N. H. L. Wang, *J. Chromatogr.*, 465 (1989) 137.
10 R. D. Whitley, J. M. Brown, N. P. Karajgikar and N. H. L. Wang, *J. Chromatogr.*, 483 (1989) 263.
11 A. Jaulmes, C. Vidal-Madjar, H. Colin and G. Guiochon, *J. Phys. Chem.*, 90 (1986) 207.
12 F. E. Regnier and I. Mazsaroff, *Biotechnol. Prog.*, 3 (1987) 22.
13 F. D. Antia and Cs. Horváth, *J. Chromatogr.*, 484 (1989) 1.
14 L. R. Snyder, G. B. Cox and P. E. Antle, *J. Chromatogr.*, 444 (1988) 303.
15 G. B. Cox, P. E. Antle and L. R. Snyder, *J. Chromatogr.*, 444 (1988) 325.
16 H. P. Jennissen, *Biochemistry*, 15 (1976) 5683.
17 A. Jaulmes and C. Vidal-Madjar, *Anal. Chem.*, 63 (1991) 1165.
18 J. A. Jönsson and P. Lövkvist, *J. Chromatogr.*, 408 (1987) 1.
19 M. W. Phillips, G. Subramanian and S. M. Cramer, *J. Chromatogr.*, 454 (1988) 1.
20 B. Lin, Z. Ma, S. Golshan-Shirazi and G. Guiochon, *J. Chromatogr.*, 500 (1990) 185.
21 B. Sébille, J. Piquion and B. Boussouira, *Eur. Pat. Appl.*, EP225829, 1987.
22 R. Lemque, C. Vidal-Madjar, M. Racine, J. Piquion and B. Sébille, *J. Chromatogr.*, 553 (1991) in press.
23 M. Czok and G. Guiochon, *Anal. Chem.*, 62 (1990) 189.
24 J. F. K. Huber and R. G. Gerritse, *J. Chromatogr.*, 58 (1971) 137.
25 R. W. Stout, S. I. Sivakoff, R. D. Ricker and L. R. Snyder, *J. Chromatogr.*, 353 (1986) 439.